

## Supporting Information

### **A novel storage to design the ultrahigh cell voltage Al-ion battery by cation- $\pi$ interactions**

Xing Liu,<sup>1</sup> Guosheng Shi,<sup>1,2\*</sup>

<sup>1</sup>*Shanghai Applied Radiation Institute and State Key Lab. Advanced Special Steel, Shanghai University, Shanghai 200444, China*

<sup>2</sup>*Division of Interfacial Water and Key Laboratory of Interfacial Physics and Technology, Shanghai Institute of Applied Physics, Chinese Academy of Sciences, Shanghai, 201800 China.*

\*E-mail: gsshi@shu.edu.cn

## CONTENTS

**PS1. Adsorption energy ( $E_{ads}$ ), average Al<sup>3+</sup>/Al-carbon distance (R), and transfer Millikan charges for the internal and external adsorption of Al<sup>3+</sup>/Al on CNT(8,8), adsorption on one graphene sheet and between two graphene sheets**

**PS2. The most stable geometry optimized structures for the internal and external adsorption of Al<sup>3+</sup> on different diameters of CNTs**

**PS3. The most stable geometry optimized structures for the internal and external adsorption of Al on different diameters of CNTs**

**PS4. The most stable geometry optimized structures of Al<sup>3+</sup> adsorption on one graphene sheet with different sizes**

**PS5. The most stable geometry optimized structures of Al adsorption on one graphene sheet with different sizes**

**PS6. The most stable geometry optimized structures of Al<sup>3+</sup> adsorption between two graphene sheets with different sizes**

**PS7. The most stable geometry optimized structures of Al adsorption between two graphene sheets with different sizes**

**PS8. Two Al<sup>3+</sup> adsorption inside and outside of CNT(8,8) and multi-ion effect on the cell voltage and adsorption energy and the capacity.**

**PS9. Different cathode electrode materials and electrolytes for Al ion batteries in experiments and theoretical calculation**

**PS10. The calculation results with the basis set of 6-311G (d,p)**

**PS11. The effect of C-C bond length after Al<sup>3+</sup>/Al adsorption**

**PS12. The change of HOMO-LOMO energy gap after Al<sup>3+</sup> adsorption on different diameters CNTs**

**PS13. The Al<sup>3+</sup> diffusion constant in different systems**

**PS14. Detailed description about calculation method and models**

**PS1. Adsorption energy ( $E_{ads}$ ), average Al<sup>3+</sup>/Al-carbon distance (R), and transfer Millikan charges for the internal and external adsorption of Al<sup>3+</sup>/Al on CNT(8,8), adsorption on one graphene sheet and between two graphene sheets**

Table S1. Adsorption energies ( $E_{ads}$ ), average Al<sup>3+</sup>/Al-carbon distance (R), and transfer Millikan charges for the internal and external adsorption of Al<sup>3+</sup>/Al on CNT(8,8), adsorption on one graphene sheet and between two graphene sheets at B3LYP/6-31G(d) level. “+” and “-” in Transfer Millikan charge represent that the Al<sup>3+</sup> and Al gains and loses electrons, respectively.

Al <sup>3+</sup> /Al@CNT/G Clusters	$E_{ads}$ (kcal/mol)	$R_{ion/atom-C}$ (Å)	Transfer Millikan Charge
Al <sup>3+</sup> @CNT(8,8)-in	-811.5	2.648	+2.461
Al@CNT(8,8)-in	-11.0	2.598	-0.537
Al <sup>3+</sup> @CNT(8,8)-out	-818.7	2.722	+2.398
Al@CNT(8,8)-out	-13.3	2.763	-0.454
Al <sup>3+</sup> @G	-851.2	2.685	+2.445
Al@G	-21.0	2.633	-0.495
G@Al <sup>3+</sup> @G	-803.6	3.039	+2.395
G@Al@G	-5.0	3.027	-0.573

The adsorption energy ( $E_{ads}$ ) is defined as

$$E_{ads} = E_{Al^{3+}/Al@CNT} - E_{CNT} - E_{Al^{3+}/Al}$$

where  $E_{Al^{3+}/Al@CNT}$ ,  $E_{CNT}$ , and  $E_{Al^{3+}/Al}$  are interaction energies of the Al<sup>3+</sup>/Al @CNT systems, the CNT, and the Al<sup>3+</sup>/Al, respectively. For Al<sup>3+</sup> adsorption on one graphene sheet and between two graphene sheets, the similar formula is used to calculate the

adsorption energy, just changing the CNT in the formula to one graphene sheet or two graphene sheets.

As showed in Table S1, the adsorption energy is 7.2 kcal/mol larger when  $\text{Al}^{3+}$  adsorbs on the external wall of CNT(8,8) than that on the internal wall of CNT(8,8), which demonstrates that  $\text{Al}^{3+}$  is more likely to adsorb on the external wall of CNT (8,8). The adsorption energy of  $\text{Al}^{3+}$  adsorption on one graphene sheet is the largest; while the adsorption energy is the smallest when  $\text{Al}^{3+}$  adsorbs between two graphene sheets. The adsorption energy of Al adsorption on the external wall is 5.6 kcal/mol larger than that on the internal wall, which shows that Al is also more likely to adsorb on the external wall of CNT(8,8). These results are consistent with that  $\text{Li}^+/\text{Li}$  prefers to adsorb on the outside wall of CNT<sup>1</sup>. The adsorption energy of Al is much smaller than that of  $\text{Al}^{3+}$ , which proves that  $\text{Al}^{3+}-\pi$  interactions is much larger than  $\text{Al}-\pi$  interactions.

**PS2. The most stable geometry optimized structures for the internal and external adsorption of  $\text{Al}^{3+}$  on different dimaters of CNTs**

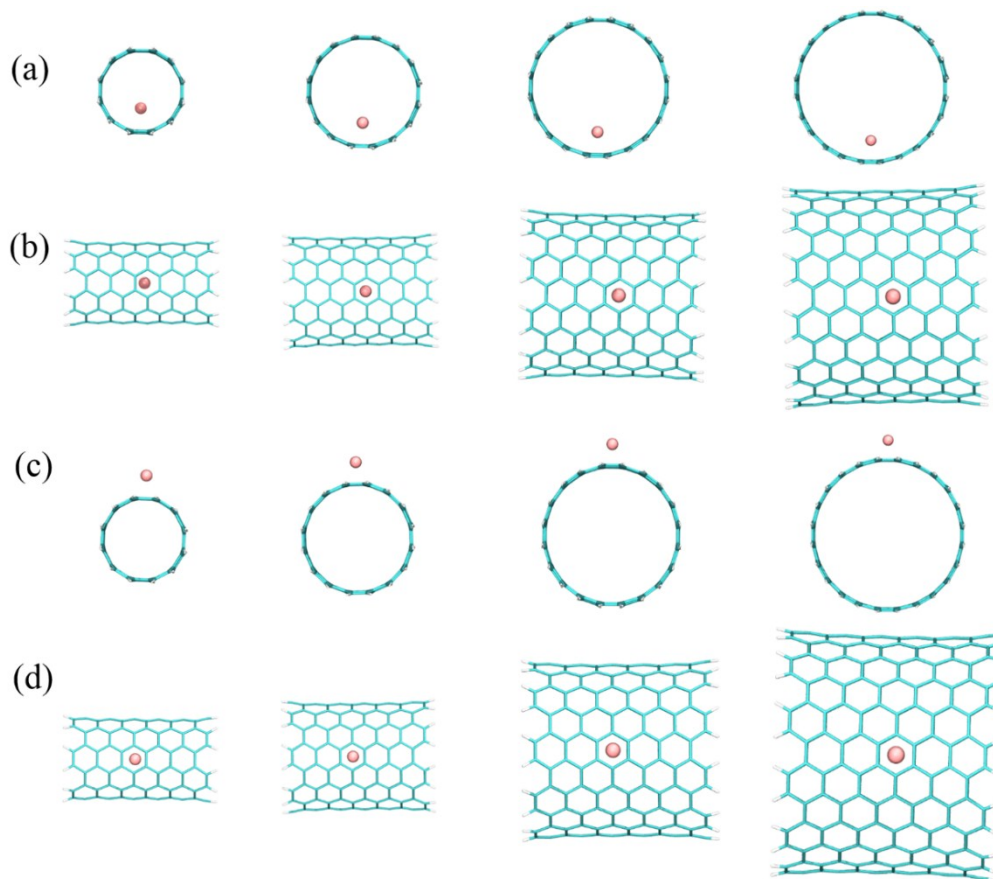


Fig. S1. Top (a) and side (b) views of  $\text{Al}^{3+}$  internal adsorption at the most stable hollow site of (6,6),(8,8), (10,10), (12,12). Top (c) and side (d) views of  $\text{Al}^{3+}$  external adsorption at the most stable site of (6,6),(8,8), (10,10), (12,12).

**PS3. The most stable geometry optimized structures for the internal and external adsorption of Al on different diameters of CNTs**

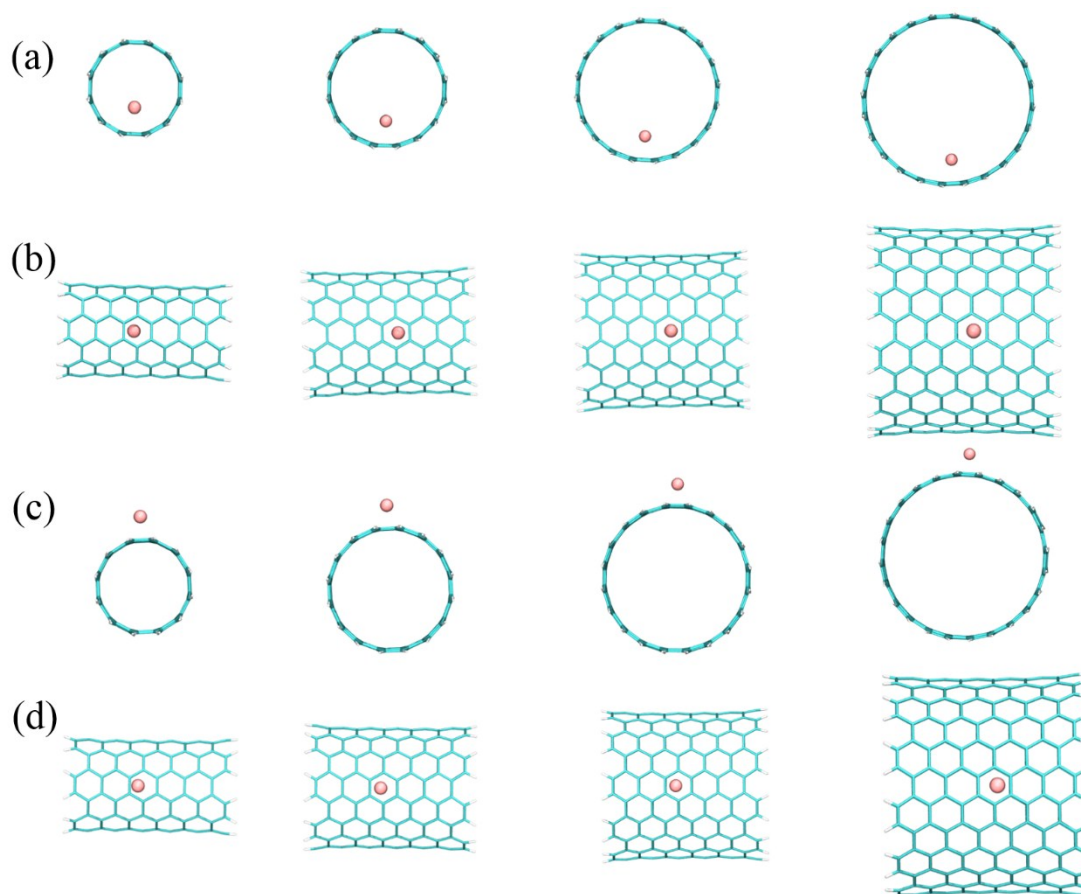


Fig. S2. Top (a) and side (b) views of Al internal adsorption at the most stable hollow site of (6,6), (8,8), (10,10), (12,12). Top (c) and side (d) views of Al external adsorption at the most stable site of (6,6), (8,8), (10,10), (12,12).

**PS4. The most stable geometry optimized structures of Al<sup>3+</sup> adsorption on one graphene sheet with different sizes**

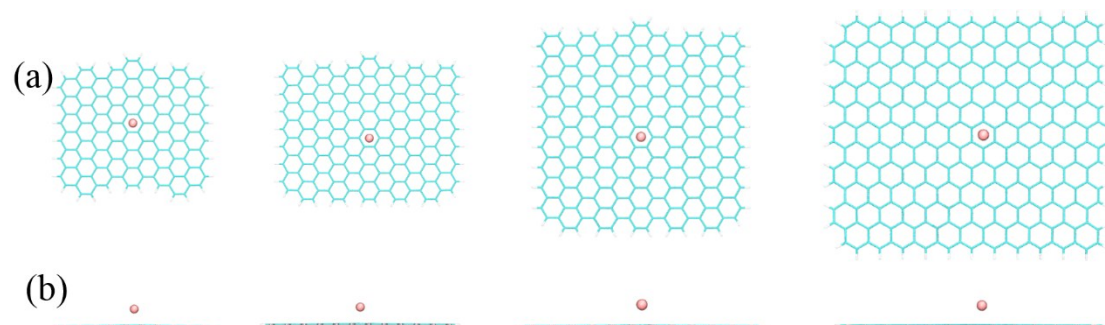


Fig. S3 Top (a) and side (b) views of Al<sup>3+</sup> adsorption on one graphene sheet with different sizes.

**PS5. The most stable geometry optimized structures of Al adsorption on one graphene sheet with different sizes**

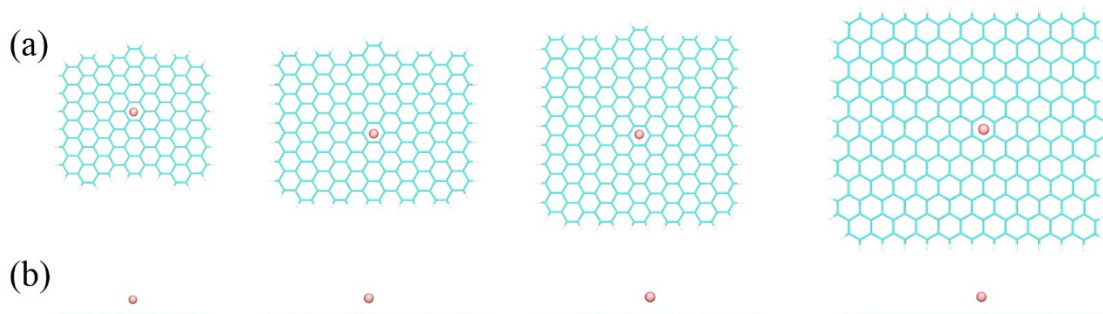


Fig. S4 Top (a) and side (b) views of Al adsorption on one graphene sheet with different sizes.

**PS6 .The most stable geometry optimized structures of Al<sup>3+</sup> adsorption between two graphene sheets with different sizes**

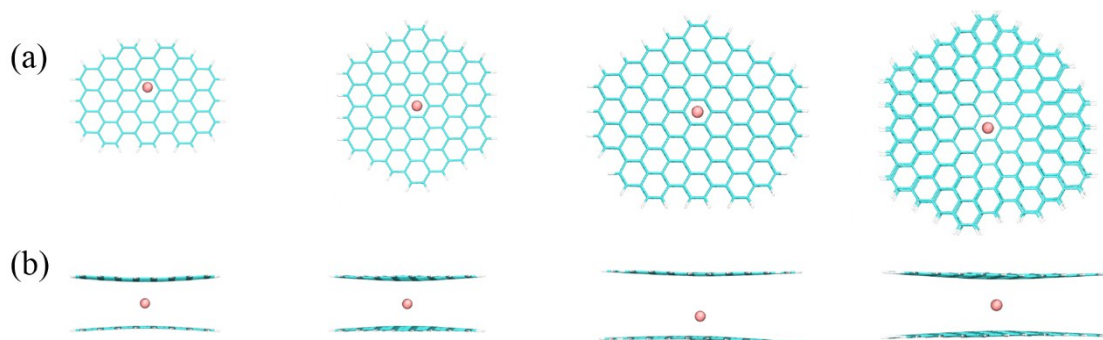


Fig. S5 Top (a) and side (b) views of Al<sup>3+</sup> adsorption between two graphene sheets with different sizes.

**PS7 .The most stable geometry optimized structures of Al adsorption between two graphene sheets with different sizes**

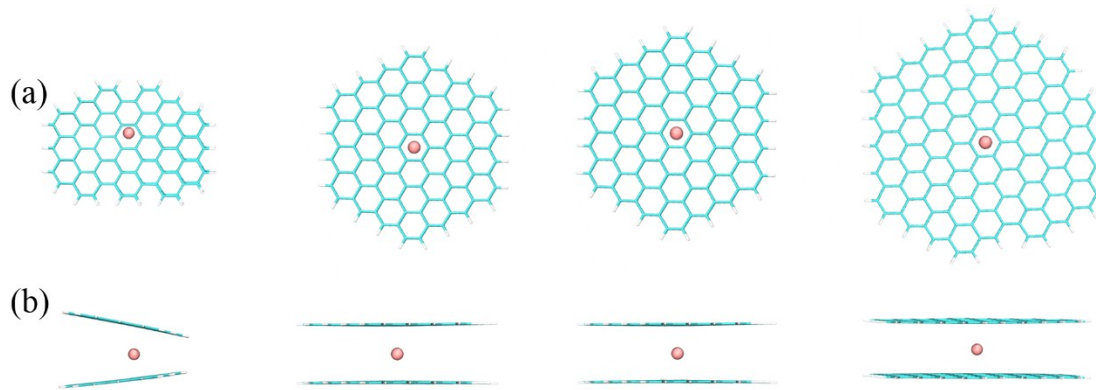


Fig. S6 Top (a) and side (b) views of Al adsorption between two graphene sheets with different sizes.

**PS8. Two  $\text{Al}^{3+}$  adsorption inside and outside of CNT(8,8) and multi-ion effect on the cell voltage and adsorption energy and the capacity.**

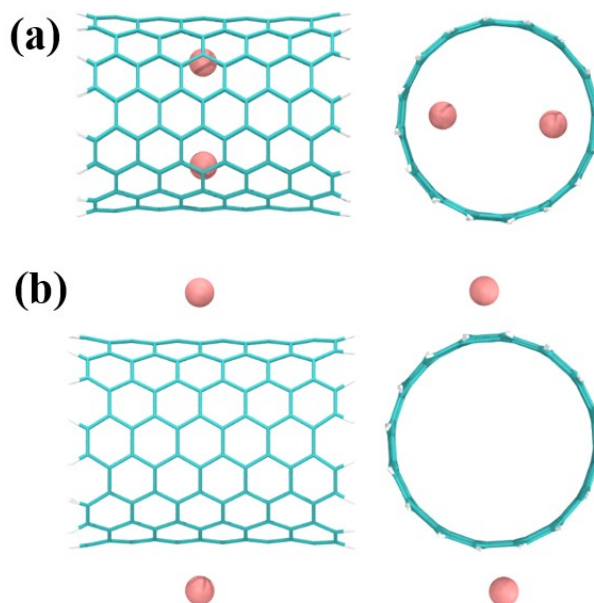


Fig. S7 Side and top views of two  $\text{Al}^{3+}$  adsorption inside (a) and outside (b) of CNT (8,8)

Table S2. The cell voltages and adsorption energy for different systems.

	Internal wall		External wall	
	$E_{ads}$ (kcal/mol)	$V_{cell}$ (V)	$E_{ads}$ (kcal/mol)	$V_{cell}$ (V)
1- $\text{Al}^{3+}$	-811.5	11.57	-818.7	11.65

2-Al <sup>3+</sup>	-1212.1	8.57	-1247.2	8.80
--------------------	---------	------	---------	------

Taking CNT(8,8) as an example, we studied two Al<sup>3+</sup>/Al adsorption inside and outside of CNT(8,8) as showed in Fig. S7. The total adsorption energy increased and the adsorption energy per atom/ion decreased when two Al<sup>3+</sup> was adsorbed inside and outside the CNT(8,8). The values of cell voltage decreased to 8 V when two Al<sup>3+</sup> was adsorbed inside and outside the CNT(8,8), which is still higher comparing to the current experiments. As the increase of Al<sup>3+</sup>/Al density, the difference of cell voltage between the external wall and internal wall is larger, as shown in Table S2. Overall, our main conclusions don't change, for example: the Al<sup>3+</sup>- $\pi$  interaction is beneficial to cell voltage and the cell voltage is larger when Al<sup>3+</sup> adsorbed on the external wall than that on the internal wall. We also note that the impact of Al<sup>3+</sup>- $\pi$  interaction on the voltage becomes complex when multiple ions intercalate into the CNTs.

To further calculate the greatest density, we performed different numbers of Al atom adsorption on the periodic CNT(8,8), as shown in Fig.S8. When the number of Al atom increase from one to four, aluminum atom can be adsorbed in the dispersive way, when the number of aluminum increase further to eight inside the CNT, aluminum atom gather together to form cluster, the minimum distance between aluminum atom in the cluster contained eight aluminum atom is 0.256 nm, which is less than the nearest distance of aluminum atom 0.286 nm in crystal structure. Outside the CNT(8,8), the density can reach AlC<sub>12</sub>. Our current results based on CNT(8,8) are smaller than the CNT-Li based batteries which can reach LiC<sub>2</sub><sup>2</sup>. As the diameter of CNT increases, the adsorption density can also may increase.

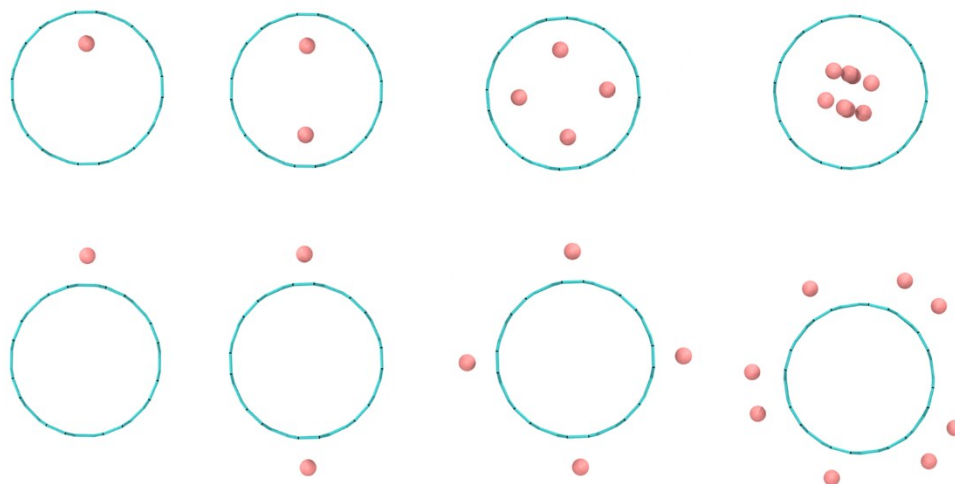


Fig. S8 The geometry optimized structures when different numbers of aluminum atom adsorption inside and outside of CNT(8,8).

We note that the specific capacity can be obtained through the formula  $C = nxF/M_f$ <sup>3,4</sup>, where  $n$  is the number of electrons transferred per formula unit,  $x$  is the number of Al atom involved,  $F$  is the Faraday constant, and  $M_f$  is the mass of formula unit AlC<sub>12</sub>. Thus the capacity can reach 470.273 mAh/g when aluminum atoms were adsorbed outside CNT(8,8).

## PS9. Different cathode electrode materials and electrolytes for Al ion batteries in experiments and theoretical calculation

Table S3 Different cathode electrode materials and electrolytes for Al ion batteries in experiments and theoretical calculation

Cathode Material	Electrolyte	Intercalated Ion	Cell Voltage (V)	Capacity (mAh/g)	Current density (mA/g)	Ref
Graphitic foam	1.3:1AlCl <sub>3</sub> :EMImCl	AlCl <sub>4</sub> <sup>-</sup>	2.0	70	4000	5
Pyrolytic graphite	1.3:1AlCl <sub>3</sub> :EMImCl	AlCl <sub>4</sub> <sup>-</sup>	2.0	65	66	5
Natural graphite powder	1.3:1AlCl <sub>3</sub> :EMImCl	AlCl <sub>4</sub> <sup>-</sup>	2.25~2.0;1.9~1.5	110	99	6
graphene aerogel	1.3:1AlCl <sub>3</sub> :EMImCl	AlCl <sub>4</sub> <sup>-</sup>	1.95	100	5000	7
GNHPG	1.3:1AlCl <sub>3</sub> :EMImCl	AlCl <sub>4</sub> <sup>-</sup>	2	123	5000	8
Large-Graphene	1.3:1AlCl <sub>3</sub> :PMImCl	AlCl <sub>4</sub> <sup>-</sup>	2	90	300	9
graphite powder	1.3:1 AlCl <sub>3</sub> :urea	AlCl <sub>4</sub> <sup>-</sup>	1.9~1.5	73	100	10
graphene film	1.3:1AlCl <sub>3</sub> :[Et <sub>3</sub> NH]AlxCl <sub>y</sub>	AlCl <sub>4</sub> <sup>-</sup>	2.3~2.0;2.0~1.5	120	400000	11
Graphite paper	1.3:1AlCl <sub>3</sub> :EMImCl	Al <sup>3+</sup> / AlCl <sub>4</sub> <sup>-</sup>	2.1	70	20	12
Li <sub>3</sub> VO <sub>4</sub> @C	1.3:1AlCl <sub>3</sub> :EMImCl	Al <sup>3+</sup>	0.5	137	20	13
Binder-free V <sub>2</sub> O <sub>5</sub>	1.1:1AlCl <sub>3</sub> :EMImCl	Al <sup>3+</sup>	0.6	239	44.2	14
VO <sub>2</sub>	1.1:1AlCl <sub>3</sub> :EMImCl, 0.5 wt% C14H14OS	Al <sup>3+</sup>	0.5	165	50	15
TiO <sub>2</sub> nanoleaves	1.0 M Al(NO <sub>3</sub> ) <sub>3</sub>	Al <sup>3+</sup>	0.95	278.1	50	16
Al <sub>x</sub> MnO <sub>2</sub> ·nH <sub>2</sub> O	5.0M Al(OTf) <sub>3</sub> -H <sub>2</sub> O	Al <sup>3+</sup>	1.1	467	30	17
Mo <sub>6</sub> S <sub>8</sub> Carbon paper	1.5:1AlCl <sub>3</sub> :BmImCl	Al <sup>3+</sup>	0.55	148	12	18
G-VS <sub>2</sub>	1.3:1AlCl <sub>3</sub> :EMImCl	Al <sup>3+</sup>		186	100	19
MoS <sub>2</sub>	1.3:1AlCl <sub>3</sub> :EMImCl	Al <sup>3+</sup>	0.8	253.6	20	20
<b>Theoretical calculation</b>						
graphite		AlCl <sub>4</sub> <sup>-</sup>	2.01~2.3	69.62		21
Graphene/hBN		AlCl <sub>4</sub> <sup>-</sup>	2.14	183		3
SWNT		AlCl <sub>4</sub> <sup>-</sup>	1.96	275		4
<b>CNT (In this paper)</b>		<b>Al<sup>3+</sup></b>	<b>~11@CNT(8,8)</b>	<b>~470</b>		

CNHP= plasma-etched graphene nanoribbons on highly porous 3D graphene foam. The blank areas are the parameters that did not report in the literature.

## PS 10 The calculation results with the basis set of 6-311G (d,p)

In order to test different basis sets effect on the calculation results, we take the system of CNT(12,12) as an example to perform the single energy calculation using the basis set 6-311 G(d,p).

As shown in Fig. S9, the cell voltage decrease slightly, but is still high ~11.9 V.

The adsorption energy of  $\text{Al}^{3+}$  decrease slightly whether the  $\text{Al}^{3+}$  was adsorbed inside or outside CNT(12,12). The adsorption energy of Al increase slightly whether the Al was adsorbed inside or outside CNT(12,12). The cell voltage of  $\text{Al}^{3+}$  adsorption outside CNT(12,12) is larger than that of  $\text{Al}^{3+}$  adsorption inside CNT(12,12), which is consistent with the result in our main manuscript (at B3LYP/6-31 G(d)).

These results indicate that different basis sets have little effect on the cell voltage, adsorption energy, the main conclusions in the manuscript are still valid.

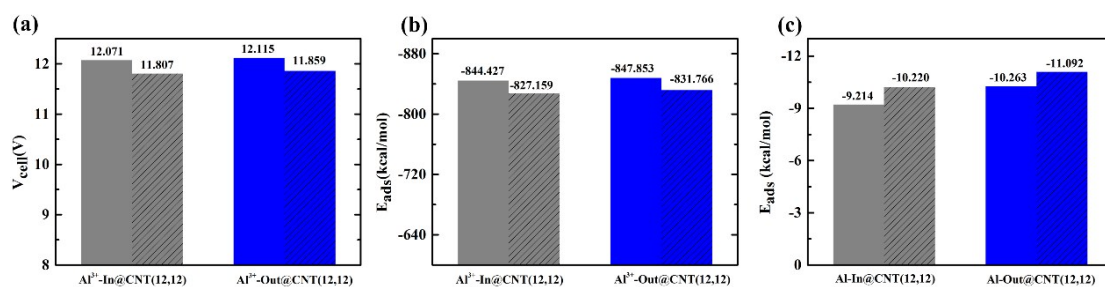


Fig. S9 (a) Cell voltage of  $\text{Al}^{3+}$  adsorption inside/outside CNT (12,12) using different basis sets. (b) Adsorption energy of  $\text{Al}^{3+}$  adsorption inside/outside CNT(12,12). (c) Adsorption energy of Al adsorption inside/outside CNT(12,12). The columns with diagonal lines stand for new calculation data with the basis set of 6-311G(d,p).

### PS11. The effect of C-C bond length after $\text{Al}^{3+}/\text{Al}$ adsorption

As listed in Table S4, we have compared the average C-C bond length of the nearest six carbon atom around the  $\text{Al}^{3+}/\text{Al}$  adsorption site on CNT/graphene with the average C-C bond of CNT/graphene without  $\text{Al}^{3+}/\text{Al}$  adsorption. The data in the bracket are the percent of bond length relaxation after  $\text{Al}^{3+}/\text{Al}$  adsorption. The percent of C-C bond length relaxation is calculated by the average C-C bond length difference with or without  $\text{Al}^{3+}/\text{Al}$  adsorption divided the average C-C bond length of CNT/Graphene without  $\text{Al}^{3+}/\text{Al}$  adsorption.

Obviously, the bond length relaxation is very small, less than 1.5%. Thus the adsorption of  $\text{Al}^{3+}/\text{Al}$  has little effect on the structure change of CNTs/graphene.

Table S4. The average C-C bond length in different systems with/without  $\text{Al}^{3+}/\text{Al}$  adsorption.

$D_{\text{C-C}}$ (nm)	Original	Al-ion-In	Al-ion-Out	Al-atom-In	Al-atom-Out
CNT(6,6)	0.142	0.144 (1.41%)	1.43 (0.70%)	0.144 (1.41%)	0.144 (1.41%)
CNT(8,8)	0.142	0.143 (0.70%)	0.143 (0.70%)	0.144 (1.41%)	0.144 (1.41%)
CNT(10,10)	0.142	0.143 (0.70%)	0.143 (0.70%)	0.144 (1.41%)	0.144 (1.41%)

CNT(12,12)	0.142	0.143 (0.70%)	0.143 (0.70%)	0.144 (1.41%)	0.143 (0.70%)
G_C144	0.142	0.143 (0.70%)	-	0.143 (0.70%)	-
G_C192	0.142	0.143 (0.70%)	-	0.144 (1.41%)	-
G_C240	0.142	0.143 (0.70%)	-	0.144 (1.41%)	-
G_C288	0.142	0.143 (0.70%)	-	0.143 (0.70%)	-
G-G_C144	0.142	0.143 (0.70%)	-	0.143 (0.70%)	-
G-G_C192	0.142	0.143 (0.70%)	-	0.143 (0.70%)	-
G-G_C240	0.142	0.143 (0.70%)	-	0.143 (0.70%)	-
G-G_C288	0.142	0.143 (0.70%)	-	0.143 (0.70%)	-

## PS 12 The change of HOMO-LUMO energy gap after Al<sup>3+</sup> adsorption on different diameters CNTs

The HOMO-LUMO energy gap  $E_g$  is calculated by the formula  $E_g = E_{\text{LUMO}} - E_{\text{HOMO}}$ , where  $E_{\text{LUMO}}$  is the energy of the lowest unoccupied molecular orbital,  $E_{\text{HOMO}}$  is the energy of the highest occupied molecular orbital. As shown in Table S5, as the diameter of CNT increased, the HOMO-LUMO energy gap increased without Al<sup>3+</sup> adsorption, while when Al<sup>3+</sup> was adsorbed inside or outside the CNT, the HOMO-LUMO energy gap decreased gradually, and finally less than that without Al<sup>3+</sup> adsorption.

We note that  $E_g$  is related to electrical conductivity<sup>22</sup>  $\sigma$

$$\sigma \propto \exp(-E_g/k_b T)$$

where  $k_b$  is the Boltzmann constant,  $T$  is the temperature,  $E_g$  is the HOMO-LUMO energy gap. The electrical conductivity increases as the decrease of  $E_g$ , thus the CNT with bigger diameter is beneficial to improve the electrical conductivity of Al ion batteries.

Table S5 The HOMO-LUMO energy gap  $E_g$  in different diameters of CNT with/without Al<sup>3+</sup> adsorption

$E_g$ (kcal/mol)	Original	Al <sup>3+</sup> -In	Al <sup>3+</sup> -Out
CNT(6,6)	21.88	33.41	33.51
CNT(8,8)	23.95	29.37	29.28
CNT(10,10)	25.01	24.97	25.03
CNT(12,12)	25.60	19.97	20.00

## PS13. The Al<sup>3+</sup> diffusion constant in different systems

We note that the diffusion constant can be estimated by formula<sup>23</sup>  $D = va^2 \exp(-E/k_b T)$  where  $E$  is the energy barrier in the diffusion pathway, and  $k_b$  and  $T$  are the Boltzmann constant and temperature, respectively,  $a$  is the lattice constant 0.245 nm.  $v$  is the frequency of ion motion. Refer to the data in literature<sup>23</sup>  $v \approx 10^{12}$  Hz, the Al<sup>3+</sup> diffusion constant is  $5.24 \times 10^{-4}$  cm<sup>2</sup>/s at room temperature when Al<sup>3+</sup> is adsorbed outside of CNT(8,8).

The data about Al<sup>3+</sup> diffusion constant along the axis direction in different systems are listed in Table S6.

Table S6 Energy barrier of Al<sup>3+</sup> diffusion in different systems and the estimated diffusion constant.

	Energy barrier (kcal/mol)	D (10 <sup>-4</sup> cm <sup>2</sup> /s)
Al <sup>3+</sup> @CNT(8,8)-In	1.811	5.37
Al <sup>3+</sup> @CNT(8,8)-Out	2.197	5.24
Al <sup>3+</sup> @G	2.820	5.04
G@Al <sup>3+</sup> @G	2.837	5.04

#### PS14. Detailed description about calculation method and models

All geometry optimization computations were performed using the standard all-electron basis set 6-31G(d), which is widely used in the computational study of nanostructured materials. All DFT calculations are carried out using the Gaussian-09 program.<sup>24</sup>

The 14-Å-long armchair type single-walled carbon nanotubes with the chiral index (6,6), (8,8), (10,10) and (12,12) are studied (Figures S1-6 in Supporting Material). The diameters of the CNTs are 8.13 Å, 10.85 Å, 13.56 Å and 16.27 Å. All dangling carbon atoms were passivated with hydrogen atoms. Initially, the Al<sup>3+</sup>/Al was located in different sites including hollow, bond and top sites, and was more stable adsorbed above the hollow site after geometry optimization, which is consistent with previous results that the hollow site above the hexagonal ring was the most stable ion adsorption site compared with the site above the C-C bond and carbon atom<sup>1,25</sup>. Thus, we optimized the geometry of Al<sup>3+</sup>/Al adsorption at the hollow site of the hexagonal ring. All atoms are free in geometry optimization. For comparison, we also built one graphene sheet and two graphene sheets models of different sizes and kept the same number of carbon atoms with different CNT diameters.

The simplified chemical reactions involved in the Al-ion battery when we consider both Al<sup>3+</sup>-π and Al-π interactions can be described as follows:



The overall reaction is represented by the following expression:



The cell voltage can be determined by the Nernst equation<sup>1, 26,27</sup>

$$V_{cell} = \frac{-\Delta G}{zF} \quad (4)$$

Where  $z$  is the charge on the Al<sup>3+</sup> in the electrolyte ( $z = 3$ ),  $F$  is the Faraday constant, and  $\Delta G$  is the change in Gibbs free energy for the chemical reaction of Al-ion battery,

$\Delta G = \Delta E + P\Delta V - T\Delta S$ . The contributions of volume effects and entropy can be negligible at 0 K,<sup>1,3,4,21, 26,27</sup> thus we can calculate the change of Gibbs free energy by computing the change of the corresponding internal energy. The change of internal energy  $\Delta E$  can be expressed as

$$\begin{aligned}\Delta E &= E_{Al} + E_{Al^{3+}@CNT} - E_{Al@CNT} - E_{Al^{3+}} \\ &= (E_{Al^{3+}@CNT} - E_{Al^{3+}}) - (E_{Al@CNT} - E_{Al})\end{aligned}\quad (5)$$

where  $E_{Al^{3+}@CNT}$ , and  $E_{Al^{3+}/Al}$  are total energies of the Al<sup>3+</sup>/Al @CNT systems, and the Al<sup>3+</sup>/Al, respectively.

## Reference

1. S. Gao, G. Shi and H. Fang, *Nanoscale*, 2016, **8**, 1451-1455.
2. J. Zhao, A. Buldum, J. Han and J. Ping Lu, *Phys. Rev. Lett.*, 2000, **85**, 1706-1709.
3. P. Bhauriyal, G. Bhattacharyya, K. S. Rawat and B. Pathak, *J. Phys. Chem. C*, 2019, **123**, 3959-3967.
4. P. Bhauriyal, A. Mahata and B. Pathak, *Chem. - Asian J.*, 2017, **12**, 1944-1951
5. M. C. Lin, M. Gong, B. Lu, Y. Wu, D. Y. Wang, M. Guan, M. Angell, C. Chen, J. Yang, B. J. Hwang and H. Dai, *Nature*, 2015, **520**, 325-328.
6. D.-Y. Wang, C.-Y. Wei, M.-C. Lin, C.-J. Pan, H.-L. Chou, H.-A. Chen, M. Gong, Y. Wu, C. Yuan and M. Angell, *Nat. Commun.*, 2017, **8**, 14283.
7. H. Chen, F. Guo, Y. Liu, T. Huang, B. Zheng, N. Ananth, Z. Xu, W. Gao and C. Gao, *Adv. Mater.*, 2017, **29**, 1605958.
8. X. Yu, B. Wang, D. Gong, Z. Xu and B. Lu, *Adv. Mater.*, 2017, **29**, 1604118.
9. L. Zhang, L. Chen, H. Luo, X. Zhou and Z. Liu, *Adv. Energy Mater.*, 2017, **7**, 1700034.
10. M. Angell, C.-J. Pan, Y. Rong, C. Yuan, M.-C. Lin, B.-J. Hwang and H. Dai, *Proc. Natl. Acad. Sci.*, 2017, **114**, 834.
11. H. Chen, H. Xu, S. Wang, T. Huang, J. Xi, S. Cai, F. Guo, Z. Xu, W. Gao and C. Gao, *Sci. Adv*, 2017, **3**, eaao7233.
12. S. Wang, S. Jiao, W.-L. Song, H.-S. Chen, J. Tu, D. Tian, H. Jiao, C. Fu and D.-N. Fang, *Energy Storage Materials*, 2018, **12**, 119-127.
13. J. Jiang, H. Li, J. Huang, K. Li, J. Zeng, Y. Yang, J. Li, Y. Wang, J. Wang and J. Zhao, *ACS Appl. Mater. Interfaces*, 2017, **9**, 28486-28494.
14. H. Wang, Y. Bai, S. Chen, X. Luo, C. Wu, F. Wu, J. Lu and K. Amine, *ACS Appl. Mater. Interfaces*, 2015, **7**, 80-84.
15. W. Wang, B. Jiang, W. Xiong, H. Sun, Z. Lin, L. Hu, J. Tu, J. Hou, H. Zhu and S. Jiao, *Sci. Rep.*, 2013, **3**, 3383.
16. Y. J. He, J. F. Peng, W. Chu, Y. Z. Li and D. G. Tong, *J. Mater. Chem. A*, 2014, **2**, 1721-1731.
17. C. Wu, S. Gu, Q. Zhang, Y. Bai, M. Li, Y. Yuan, H. Wang, X. Liu, Y. Yuan, N. Zhu, F. Wu, H. Li, L. Gu and J. Lu, *Nat. Commun.*, 2019, **10**, 73.
18. L. Geng, G. Lv, X. Xing and J. Guo, *Chem. Mater.*, 2015, **27**, 4926-4929.

19. L. Wu, R. Sun, F. Xiong, C. Pei, K. Han, C. Peng, Y. Fan, W. Yang, Q. An and L. Mai, *Phys. Chem. Chem. Phys.*, 2018, **20**, 22563-22568.
20. Z. Li, B. Niu, J. Liu, J. Li and F. Kang, *ACS Appl. Mater. Interfaces*, 2018, **10**, 9451-9459.
21. P. Bhauriyal, A. Mahata and B. Pathak, *Phys. Chem. Chem. Phys.*, 2017, **19**, 7980-7989.
22. N. Kosar, M. Asgar, K. Ayub and T. Mahmood, *Mat. Sci. Semicon. Proc.*, 2019, **97**, 71-79.
23. V. Meunier, J. Kephart, C. Roland and J. Bernholc, *Phys. Rev. Lett.*, 2002, **88**, 075506.
24. M. Frisch, G. Trucks, H. B. Schlegel, G. Scuseria, M. Robb, J. Cheeseman, G. Scalmani, V. Barone, B. Mennucci and G. Petersson, *Gaussian 09*, revision A.1, Gaussian Inc., Wallingford, CT, 2009.
25. J. Li, H. Li, X. Liang, S. Zhang, T. Zhao, D. Xia and Z. Wu, *J. Phys. Chem. A*, 2009, **113**, 791-796.
26. M. Aydinol, A. Kohan, G. Ceder, K. Cho and J. Joannopoulos, *Phys. Rev. B: Condens. Matter Mater. Phys.*, 1997, **56**, 1354.
27. M. Aydinol, A. Kohan and G. Ceder, *J. Power Sources*, 1997, **68**, 664-668.